Renewable Energy 256 (2026) 124234

Contents lists available at ScienceDirect

Renewable Energy

journal homepage: www.elsevier.com/locate/renene

Effects of groundwater flow on end-temperature of closed-loop systems used for cooling

Simona Adrinek *, Joerg Prestor, Simona Pestotnik, Nina Rman

Geological Survey of Slovenia, Dimičeva Street 14, 1000, Ljubljana, Slovenia

ARTICLE INFO

Keywords:
Shallow geothermal energy
Cold storage facility
Intergranular aquifer
Heat load
Groundwater flow
Slovenia

ABSTRACT

Stable subsurface temperatures provide a reliable source of shallow geothermal energy. This research is one of a few that investigates the potential of closed-loop systems for cold storage facilities. We listed 47 cold storage facilities in Slovenia and evaluated the capacity of two 50 m deep borehole heat exchangers that would penetrate one of five intergranular aquifers. As the Slovenian legislation does not define temperature thresholds of the heat carrier fluid, we applied – 3 °C and +24 °C as conservative boundary conditions. First, we quantified the possible amount of injected waste heat with the analytical model (EED) using seven scenarios. Further, we upgraded our results with the three scenarios in the numerical model (FEFLOW), including groundwater flow. The calculation revealed that the optimal natural conditions for geothermal cooling of cold storages are in the Sava Basin, where fast groundwater flow (7.2 m/day) increases possible injected heat in numerical calculation to more than 900 % compared to analytical calculation. Cooling capacities decrease from the Sava to Drava, Mura, Savinja and Krško Basins. Our research quantitatively confirms that areas with groundwater flow are more conductive to restoring underground temperatures through the injection of waste heat from cooling cold storages than areas without groundwater flow.

Abbreviations and symbols

Symbol/Abbreviation	Meaning	Unit
c_v	Volumetric heat capacity of underground	MJ/(m^{3}K)
c_{eff}	Effective volumetric heat capacity	MJ/(m^{3}K)
D_{nez}	Thickness of unsaturated layers	m
D_{vod}	Thickness of aquifer/saturated layers	m
D_{pod}	Thickness of rocks	m
HF	Heat flow density	W/m^2
i	Hydraulic gradient	–
k	Hydraulic conductivity	m/s
n	Porosity	–
Pe	Peclet number	–
T_z	Air temperature	°C
T_0	Ground surface temperature	°C
T	Temperature	°C
v	Groundwater velocity	m/day
λ	Thermal conductivity	W/mK
λ_{eff}	Effective thermal conductivity	W/mK
α	Thermal diffusivity	m^2/s
ρ_w, c_w	Water density and specific heat	/
ρ_s, c_s	Solid matrix density and specific heat	/
Q_T	Heat source/sink	W/m^3
BC	Boundary Condition	/
BHE	Borehole Heat Exchanger	/
COP	Coefficient of performance	/
EED	Earth Energy Designer software	/
FEM	Finite Element Method	/
G	Grout temperature	/
PI	Pipe-In temperature	/
PO	Pipe-Out temperature	/
ΔT(t)	Temperature increase at time t	°C
t	Time since heat injection/extraction began	s
H	Borehole depth	m
z, z'	Integration variables along borehole depth	m

1. Introduction

Shallow geothermal energy (SGE) is one of the renewable energy sources that has minimal impact on the environment when properly utilized [1]. It is a reliable and constant source of low-carbon renewable

This article is part of a special issue entitled: Geothermal heating-cooling published in Renewable Energy.

* Corresponding author.
E-mail address: simona.adrinek@geo-zs.si (S. Adrinek).

https://doi.org/10.1016/j.renene.2025.124234
Received 18 December 2024; Received in revised form 5 August 2025; Accepted 12 August 2025
Available online 13 August 2025

heat that is not dependent on weather conditions. Stable subsurface temperatures throughout the year allow for predictable use of SGE for both, heating and cooling [2,3]. The disadvantage of SGE is rather high investment cost, which depends on local natural conditions and energy demand [1,4,5]. SGE are divided into open- and closed-loop systems (Fig. 1). In the first, heat is extracted from or injected into via at least two wells – pumping and injection wells [2]. The closed-loop system extracts or injects heat using heat exchangers embedded in the ground. The heat or cold is transported by a fluid circulating in the heat exchanger pipe and transferred to a heat pump on the surface [1].

Many review articles discuss the world use of SGE [6–8]. The authors provide a comprehensive overview of heating and cooling, including natural and technical characteristics, system optimization, and modeling.

Larsen et al. [9] highlighted that in Europe, where heating demand will generally decline due to climate change, cooling demand will increase by 25–50 % between 2010 and 2050. The International Energy Agency (IEA) came to a similar conclusion, indicating that the demand for cooling will increase by over 3 % annually over the next three decades, eight times faster than the demand for heating over the last 30 years [10].

In agriculture, the utilization of SGE is not so widespread as, traditionally, the greenhouses are provided with thermal water. Still, more and more greenhouses are heated or cooled also by SGE [11–13]. Sparse research is focused on SGE providing cool for cold storage facilities for perishable foods. Niemann et al. [14] investigated an air conditioning system during summer and winter. The system employed desiccant-assisted dehumidification and enthalpy recovery, as well as a SGE unit for cooling and heating.

Singh et al. [15] implemented a geothermal loop within the condenser section of a refrigeration system which resulted in a reduction of sink temperature and water consumption within a potato cold storage facility in India. This resulted in a reduction of condenser temperature by about 10–15 °C, which increased the COP of the refrigeration system. Many cold stores are designed to accommodate a temperature range of around 2–3 °C, which is optimal for the cold stores of potatoes. However, the lack of suitable storage facilities for other agricultural products, such as fruit and seasonal vegetables, represents a significant limitation. The utilization of a cascaded vapor compression refrigeration system can result in a reduction in energy consumption and the provision of a range of temperatures for the storage of a variety of foods. Pastakkaya [16] showed that a geothermally driven absorption cooling system in the cold storage of apple fruit can meet its cooling requirements on an annual basis. Furthermore, it facilitates safer and more cost-effective cooling solutions with a comparable cooling capacity to alternative sorption cooling systems. Galgaro et al. [17] presented an experience with apple cold storage in an abandoned dolomite mine in Italy where an open-loop system provides needed cooling.

The number of shallow geothermal units (individual heat pumps) in Slovenia has risen steadily by around 8.8 % in the last 10 years [18]. Based on annual budget evaluation prepared by the Geological Survey of Slovenia, there were 17,369 units at the end of 2023. Approximately 1433.83 TJ (398.29 GWh) of heat was extracted from the subsurface, with at least 360 TJ/year of heat being injected due to cooling demand [18].

A review of the literature on cold storage facilities in Slovenia showed a lack of systematic research, with the majority focusing on the storage of fruit. A review of cold storage facilities was conducted in 1991 [19], while later publications mainly covered e.g. the possibilities of using the waste heat of the fruit cold storage [20], the methods of upgrading the apple cold storage [21], the control of the atmosphere in the cold storages [22], the economic analysis of the fruit cold storage [23] and the eligibility criteria for fruit logistics centers and vegetables [24]. Research has also been conducted on the biological changes in apples during cold storage [25].

From a hydrogeological perspective, cold storage facilities in Slovenia are predominantly situated at flatlands of Quaternary alluvial valleys where unconfined intergranular aquifers with high groundwater

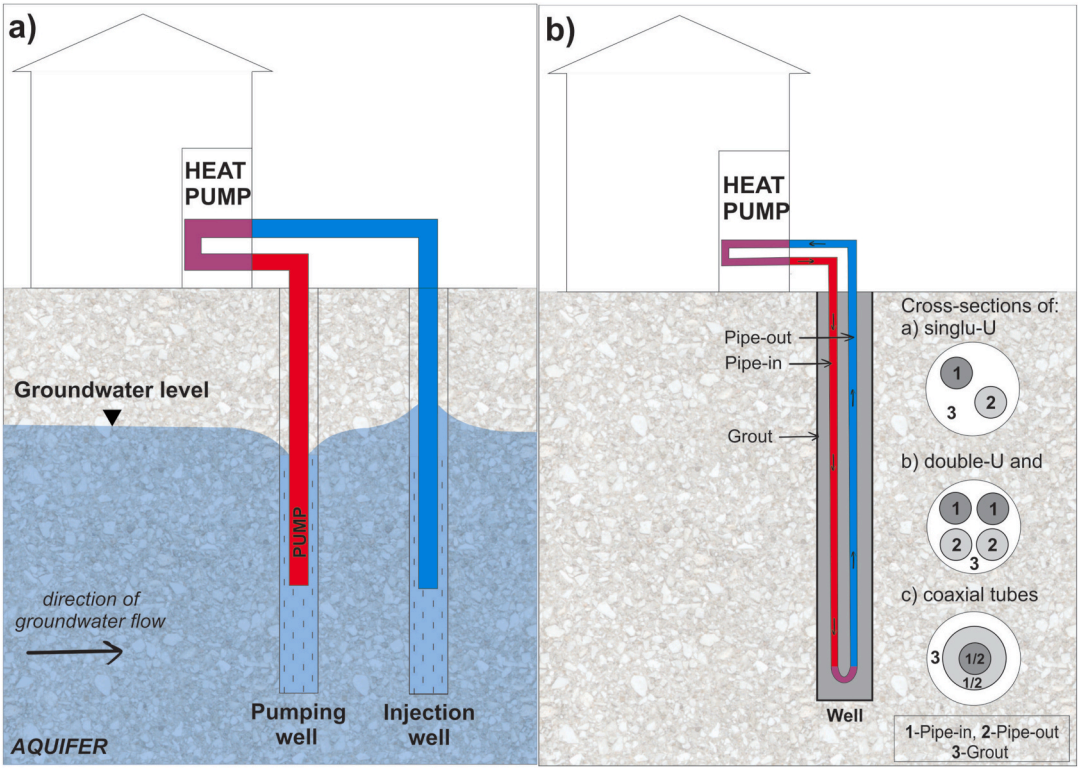

Fig. 1. a) Scheme of an open-loop system (heating mode) and b) Scheme of a vertical closed-loop system (cooling mode) with cross-sections of various distributions of heat exchangers.

flow prevail. Banks [1] reported that groundwater flow has a significant impact on temperature distribution at boreholes and their performance. As it enhances subsurface apparent thermal conductivity and heat transport, shorter BHEs and therewith lower installation costs are expected [2,26].

The use of numerical models to simulate the propagation of thermal plumes is increasingly used as a decision-support tool for the management of shallow geothermal resources [27–31]. Chiasson et al. [32] investigated the influence of groundwater flow on a single closed-loop heat exchanger in various geologic materials. Their findings revealed that the advection of heat by groundwater flow significantly enhances heat transfer in geologic materials with high hydraulic conductivity, such as sands, gravels, and rocks exhibiting fractures and solution channels. Angelotti et al. [33] made a numerical model in MODFLOW/MT3DMS of a single U-pipe in a sandy aquifer. They found out that for Peclet number (*Pe*) in the range between $0.1 \leq Pe \leq 1$, cold and warm plumes develop and the heat rate increases non-linearly from 11 % to 105 %. Dehkordi and Schincariol [34] showed the importance of subsurface thermal conductivity, groundwater flow (velocity $>10^{-7}$ m/s), background temperature, and inlet temperature on the performance and impact of the system. They simulated the thermal plumes that evolve asymmetrically in the presence of groundwater flow, forming a cold thermal plume that do not restore during the 25 year operational period. Deng et al. [35] propose that thermal imbalance should be allowed during the operation of shallow geothermal systems, which can be compensated for by appropriate use of groundwater heat replenishment in other seasons, achieving thermal balance year-round. Previati and Crosta [36] showed how a trained model can be used to predict the geothermal potential of SGE for almost all sedimentary basins upon the availability of the required input data (aquifer thickness and saturation, aquifer porosity, and groundwater flow velocity). In their study, large-scale geothermal potential maps were generated for the area in northern Italy, showing highly variable groundwater flow (Darcy velocity from 10^{-3} to 10^{+3} m/y). A promising increase (up to +250 %) in the heat exchange potential of shallow geothermal systems due to the contribution of advection was highlighted, and the benefits of groundwater flow and the amount of usable potential were discussed. Concerning the closed-loop system, it is important to consider not only the hydrogeological conditions but also the thermal conditions in the subsurface. These can be influenced by the injection of waste heat. Bonte et al. [37] investigated the impacts of subsurface cold and heat storage on chemical and microbiological status. They highlighted that heating the subsurface from the original 11 °C to an end temperature of 25 °C and more (as it is expected with cold storage use) already impacts both. Changes become more and more pronounced with increasing temperature. A study by Griebler et al. [38] demonstrated that a moderate increase in groundwater/aquifer temperature (5 to 10 °C) typically results in only minor changes in water chemistry, microbial biodiversity, and ecosystem functions in uncontaminated and low-energy groundwater systems. In aquifers contaminated with organic matter, nutrients, and heavy metals, which are typically found in urban areas and sites with intensive land use (e.g., agriculture), and especially at injected temperatures ≥30 °C, significant changes in water quality and ecological patterns can occur.

In most countries, there are no regulations or recommendations on temperature limits for the use of the shallow subsurface [39,40] despite possible effects on chemical and microbiological conditions. Only a few countries, such as Austria, have defined their technical temperature thresholds, defining the temperature limits of the heat carrier fluid. In Austria, the technical thresholds are ±15 °C for temperature difference and 35 °C for maximum injection temperature. The minimum temperature is set at 0 °C for the weekly average load and −5 °C if the peak load is included. In France, there are no explicit temperature limits in place. However, their Water Act sets a liberal temperature limit of 11 K for the change in groundwater temperature. In Slovenia, there is no legislation defining the minimum and maximum temperature limits for heat carrier fluid nor geological media around shallow geothermal systems.

The hypothesis of our research was that the intergranular aquifer with active groundwater flow increases the amount of waste heat that can be injected into the subsurface from cooling cold stores, compared to areas without groundwater. Therefore, the main aim of this research was to define the analytically calculated maximum injected waste heat and improve it with numerical calculation, including groundwater flow for five representative Slovenian aquifers.

2. Methodology and methods

The identified locations of cold storage facilities in Slovenia were used for selecting five representative hydrogeological settings for analysis. The results of analytical and numerical modeling are presented and the determination of the maximum amount of waste heat that can be injected is discussed.

2.1. Case study locations

Firstly, the locations of existing cold storage facilities at farms were identified with the assistance of regional agricultural consultants. We did not collect information on industrial or commercial cold storage, focusing only on those managed by individual farmers or local farmer associations. Also, we searched for sites where vegetables or fruit were stored, meat storage was not of interest. A total of 47 facilities were identified in Slovenia, of which 15 are reported to be utilized for the cool storage of vegetables, and 16 for the storage of fruits (both together sum to 31 facilities). The remaining ones (16 facilities) did not report their purpose (Fig. 2).

When planning a closed-loop system, it is important to accurately define the thermal conductivity, thermal diffusivity, and volumetric heat capacity of underground [2]. For most sediments, the volumetric heat capacity and thermal diffusivity remain relatively constant, whereas the thermal conductivity usually varies and thus requires more attention. For 31 locations identified, data on geothermal parameters were collected from existing maps (Table 1) [42–46].

Among cold storage facility locations (31 locations), we identified 19 % positioned at the areas without significant groundwater flow. Others are located at alluvial plains where groundwater flow can have a considerable impact on heat transfer and generate thermal plumes. Their size can vary depending on the hydrogeological conditions and the operational mode of the closed-loop system, i. e. whether it is used for heating or cooling [47]. The threshold for defining the thermal plume is usually set at an isotherm that has a 1 K difference from the natural background temperature [48].

Based on the data, five conceptual models were developed to represent the intergranular groundwater bodies present in the alluvial plains of the Sava, Savinja, Krško, Drava and Mura River basins (Fig. 3). These models were established using typical representative geological, hydrogeological, and geothermal parameter values [41,43,45].

2.2. Analytical modeling

Analytical modeling was performed using the Earth Energy Designer (EED), which is a software solution for dimensioning and optimizing the number, length, and mutual arrangement of vertical closed-loop systems [49]. It considers the geothermal parameters of the soil, the parameters of the device, the properties of the working fluid, and the energy requirements of the building. The software allows the user to check whether the installed vertical closed-loop system can provide the requisite heating and cooling needs or hot sanitary water. The program does not consider the convection of heat transfer, therefore, it is conservative in areas with groundwater flow. The program uses the Finite Line Source equation that describes the temperature increase at the borehole wall over time due to the constant heat injection or extraction along a finite vertical borehole [50,51] written as:

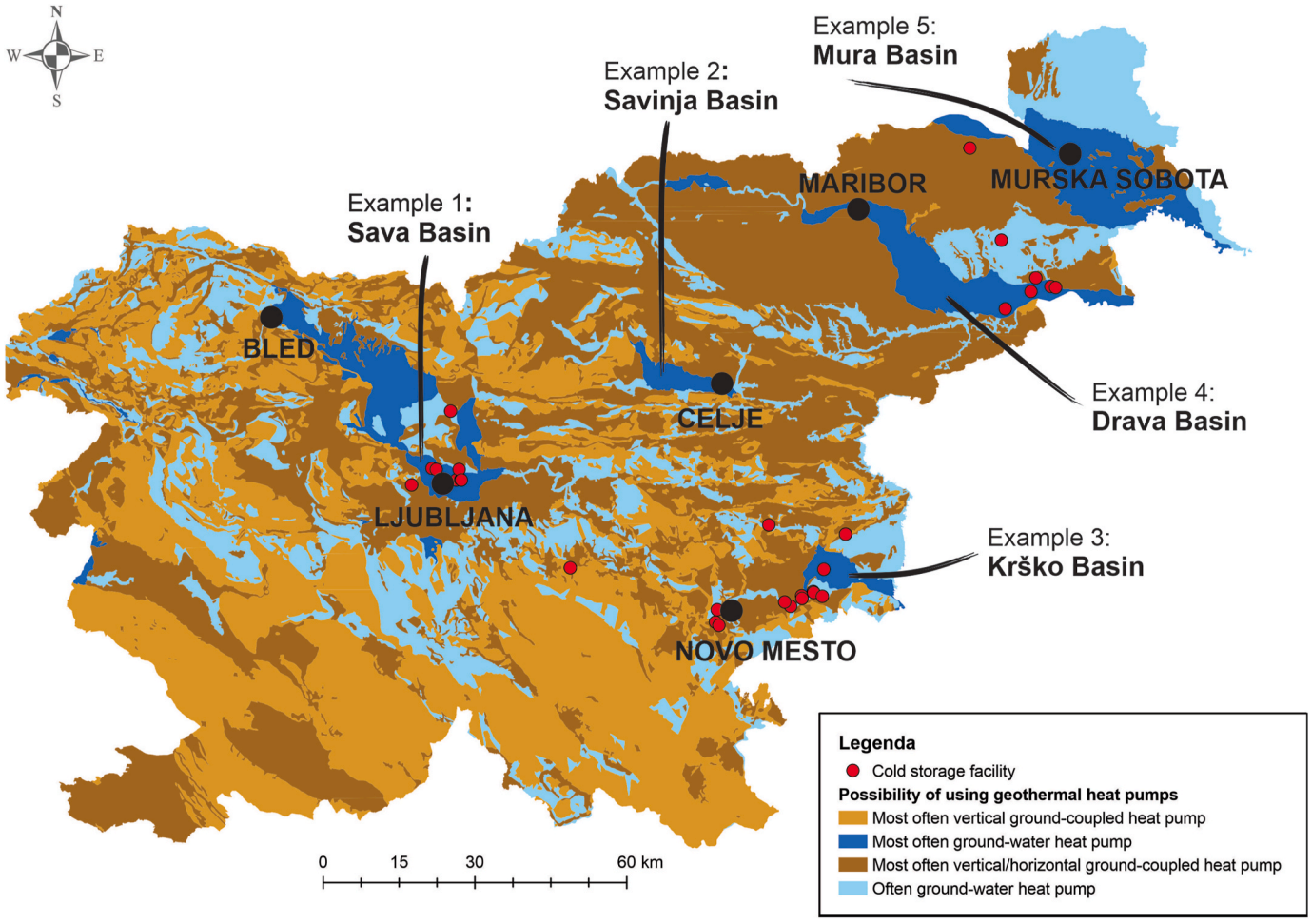

Fig. 2. Identified locations of 31 cold storage facilities, which are used either for vegetables or fruit. Sites without known types of stored food were excluded. Background map is the Map of the possibility of using geothermal heat pumps [41].

Table 1
Geothermal statistical parameters at selected 31 locations, as interpreted from geothermal maps [42–46].

Statistical parameter	Expected temperature at a depth of 100 m (°C)	Temperature on the surface of solid ground (°C)	Surface heat flow (mW/m^2)	Thermal conductivity of the uppermost geological layers (W/mK)	Volumetric heat capacity of the uppermost geological layers (MJ/m^{2}K)
Minimal value	11	11	44	0.6	1.5
Maximum value	18	12	100	4.1	2.4
Geometric mean	14	12	71	1.8	2.3
Median	14	12	78	1.7	2.3

$$\Delta T(t) = \frac{q}{4\pi\lambda}\int_0^H \int_0^H \frac{1}{\sqrt{4\alpha t}} exp\left(-\frac{(z-z')^2}{4\alpha t}\right) dz\, dz' \quad (1)$$

For analytical modeling, a 30-year simulation of using the vertical closed-loop system was conducted, with the start of operation in January. The average values of thermal conductivity and ground temperature were determined based on the locations of agricultural land in Slovenia, which were analysed in another study [52]. Since the most common combination between soil temperature and thermal conductivity (33 % of all areas) had the values $T_0 = 12$ °C and $\lambda = 1.6$ W/mK, we used these values. These values are the only ones that were different in the numerical modeling, where we set different λ and c_v for individual layers, as shown on Fig. 3. The heat flow density value was obtained from the map created by Rajver [42] and is presented in the figure (Fig. 3) for each area.

The input data of the BHE geometry and heat carrier fluid are in the table (Table 2). The heat carrier fluid used was 25 % monoethylenglycol. The temperature of the heat carrier fluid was simulated for two BHEs with a depth of 50 m. This represents a typical representative depth in most of the investigated aquifers and we wanted to target only the saturated subsurface.

The energy consumption profile for cooling was estimated based on the meteorological stations that have prepared data for the reference year [53]. The percentages used are shown in the table (Table 3). Based on the reference meteorological station data [53], we have set a conservative value for the heat input of 33,455 kWh, which could cover the demand for cooling an average cold store in Slovenia to 5 °C. From an economic point of view, this is already a number that represents a favorable and meaningful investment in Slovenia. The seasonal performance factor (SPF) for cooling was set at 3.5, the lowest and

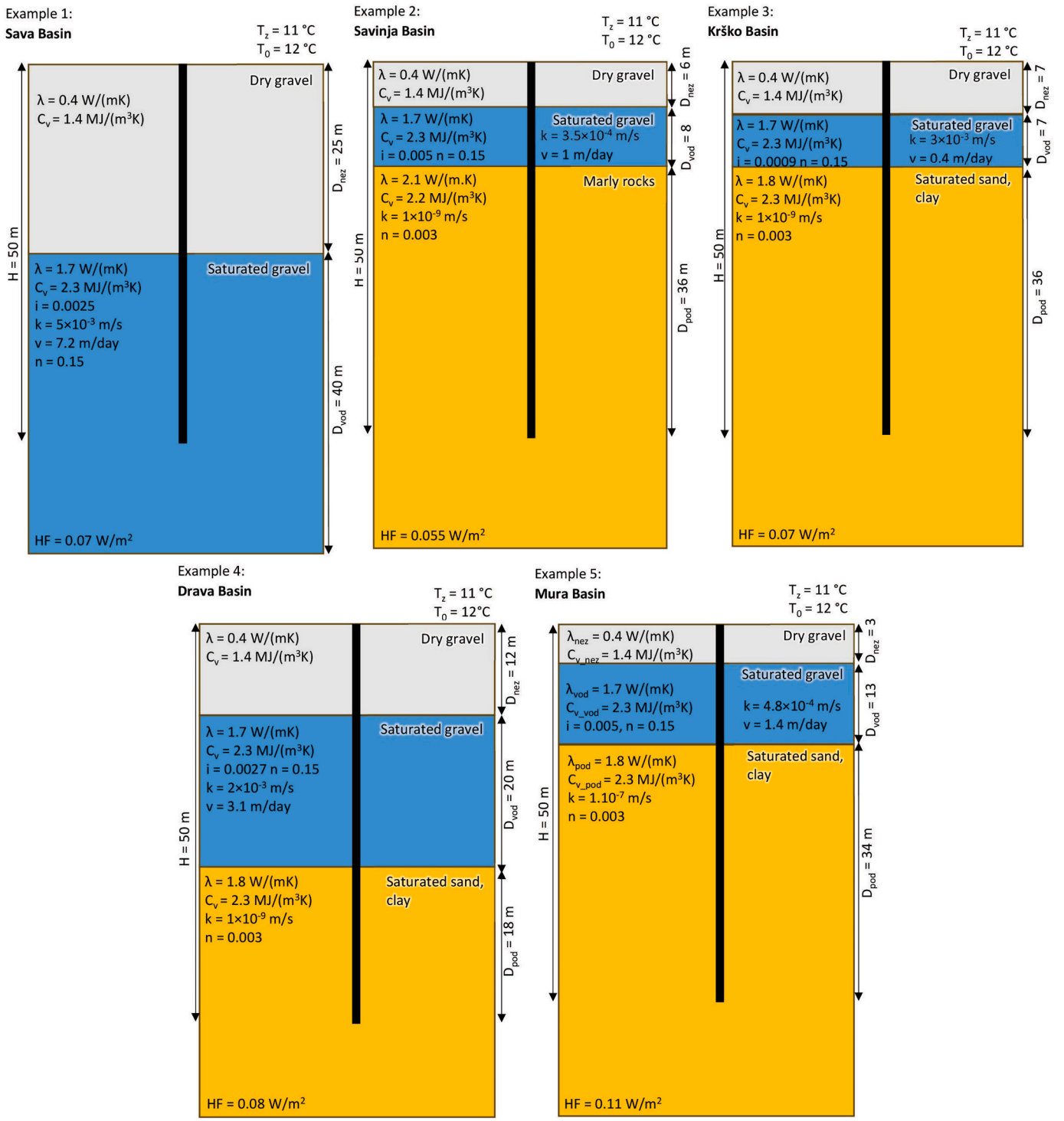

Fig. 3. Conceptual models of five Slovenian representative intergranular aquifers with the main input parameters and boundary conditions for analytical and numerical modeling. All closed-loop systems are 50 m deep.

conservative value for the use based on the market. During the simulation, the limitations of the minimum temperature of the heat carrier fluid, which was set at −3 °C, and the maximum temperature, which was set at 24 °C, were considered for average monthly loads. This temperature limitation is expected to retain good chemical and microbiological conditions of the subsurface.

The aim of the EED simulations was not to optimize the BHE configuration (i.e., number and depth), but rather to assess whether the proposed amount of heat could be injected using two 50 m BHEs. Since this was not feasible, the next step was to simulate the maximum amount of heat that could be injected under the given conditions. Additionally, due to the presence of groundwater flow, we enhanced our analysis with numerical simulations that also account for convective heat transfer. The used values and boundary conditions of these simulations are presented in the following chapter.

Table 2
Technical parameters of borehole, U-pipe and heat carrier fluid.

Technical parameter of borehole	Double U
Depth (m)	50 × 2
Spacing (m)	7
Diameter (mm)	152.0
Filling thermal conductivity (W/mK)	2.0
Flow rate (l/s)	0.5
Technical parameters of U-pipe	
Outer diameter (mm)	32
Wall thickness (mm)	3
Pipe thermal conductivity (W/mK)	0.42
Shank spacing (mm)	76
Technical parameters of heat carrier fluid	**25 % Monoethylenglycol**
Thermal conductivity (W/mK)	0.48
Specific heat capacity (J/kgK)	3795
Density (kg/m^3)	1052
Viscosity (kg/ms)	0.0052
Freezing point (°C)	−14.0

Table 3
Percentage of the cooling needed throughout the representative year. The sum equals 100 %, and the monthly percentage corresponds to an energy consumption of 33,455 kWh.

Month	Sava Basin — Ljubljana	Savinja and Drava Basin — Maribor	Krško Basin — Črnomelj	Mura Basin — Murska Sobota
January	0.5 %	0.8 %	1.0 %	0.6 %
February	0.1 %	0.3 %	0.3 %	0.3 %
March	3.1 %	2.6 %	2.9 %	2.8 %
April	5.8 %	6.7 %	6.9 %	6.9 %
May	13.7 %	13.6 %	13.8 %	13.7 %
June	17.5 %	16.5 %	15.3 %	16.7 %
July	18.5 %	20.2 %	19.1 %	19.6 %
August	17.8 %	18.1 %	17.1 %	17.6 %
September	11.3 %	10.9 %	11.2 %	11.7 %
October	7.6 %	6.7 %	7.6 %	6.2 %
November	3.2 %	2.7 %	3.5 %	3.1 %
December	0.9 %	0.9 %	1.5 %	0.8 %

2.3. Numerical modeling

Modeling was performed with the use of the FEM (Finite Element Method) numerical code FEFLOW version 8.1, using the coupled heat transport and fluid flow equation [54] defined as:

$$c_{eff}\frac{\partial T}{\partial t} + \rho_w c_w \nu \times \nabla T = \nabla \times \left(\lambda_{eff}\nabla T\right) + Q_T \quad (2)$$

A steady-state groundwater flow and heat transfer simulation was performed to define the initial conditions with fixed boundary conditions and material properties for each area as given in case studies. The aquifer was simulated as unconfined with an upper phreatic layer, which allows for the possibility of the elements in this layer becoming dry or partially saturated [54]. The Darcy equation was used for the remaining layers. The resulting hydraulic head and temperature distribution formed the basis for further transient simulations of temperature distributions.

All numerical models have dimensions of 500 m in length, 200 m in width, and 65 m in depth. In general, each numerical model comprised 13 layers and 14 slices, with a vertical distribution of 5 m. The vertical division of the model into layers was implemented to enhance the resolution of the heat exchange simulations around the closed-loop system. Following the typical groundwater level, as illustrated in the conceptual models (Fig. 3), an additional slice was incorporated into the individual model to define the hydraulic gradient of each area. The material properties assigned to the layers are presented in Fig. 3.

The discretisation of the study area was performed with a triangular algorithm. The refinement of the mesh was conducted in the vicinity of the vertical closed-loop system. The maximum side length for the elements directly at the refined point was set to 0.2 m. To reduce truncation errors during the numerical computation and to enhance the convergence behaviour of the model, the finite-element mesh was smoothed three times. The Dirichlet boundary condition (BC) was set at the northern and southern boundaries in accordance with the hydraulic gradient of the individual basins (Fig. 3). The eastern and western boundaries were set as no-flow boundaries. The undisturbed ground temperatures, as presented in Fig. 3, were used as a Temperature BC at the upper boundary of the model and on the northern border of the aquifer slices for both the static and dynamic simulations. At the bottom of the model, a constant geothermal heat flux was defined as a Neumann BC (Fig. 3). A borehole heat exchanger BC was used at two locations, indicating two 50 m boreholes. The technical characteristics of the BHE geometry and heat carrier fluid are identical to those used in the analytical modeling with EED. In the FEFLOW, we assigned these properties through the Borehole Heat Exchanger BC (Table 2, Table 3). This BC uses the BHEs as embedded 1D elements, which are linked to the mesh nodes along edges in a 3D model [55]. The same BC was used to define the inlet temperature of the heat carrier fluid. The latter were done through the monthly time series for the cooling demand (heat output rate) over the 30-year simulation period, with the flow rate set as 0.5 l/s (Table 3). As we were modeling the long-term simulation, we used the quasi-stationary approach, based on the work of Eskilson & Claesson [56], which always assumes thermal equilibrium of the BHE internal temperatures. This simplification is useful due to a higher efficiency and stability of the numerical model than the fully transient approach. The influence of groundwater flow on the maximum possible injected heat was investigated through three scenarios performed for each case study location:

- SC1 – annual energy loads as obtained with scenario 8 in analytical modeling,
- SC2 – maximum heat carrier fluid temperature set at 24 °C,
- SC3 – maximum annual energy load set on 33,455 kWh.

Before conducting a heat simulation in a transient state (30-year simulation), a steady-state simulation of groundwater flow and heat transfer was performed to establish the initial conditions in each case study area (Fig. 4). We can observe different static temperature distributions related to the assigned heat flux at the bottom of the model and the thickness of the aquifer zone (Table 1, Fig. 3). The latter is important because we have assumed a constant groundwater temperature upstream of the aquifer zone in the model. The highest temperatures are observed in the Mura Basin (Fig. 4e), because the geothermal heat flux is highest there. In contrast, the constant temperature distribution is visible in the Sava Basin (Fig. 4a), where most of the model is located in the aquifer zone and is therefore influenced by the assigned groundwater temperature.

3. Results and discussion

3.1. Analytical modeling

The specific heat injection rate was determined through analytical calculations, which considered the influence of various natural conditions, and the same technical characteristics and the typical monthly energy profile (Fig. 5), without groundwater flow.

One of our aims was to test whether it would be possible to inject 33,455 kWh into the ground without exceeding a temperature of 24 °C. If this was not achieved, we gradually reduced the amount of heat injected, resulting in eight different scenarios with varying levels of injected heat. These included 33,455 MWh, 33 MWh, 30 MWh, 25 MWh, 20 MWh, 15 MWh, 10 MWh, and the final scenario with various injected values. With the eighth scenario, we determined the maximum amount

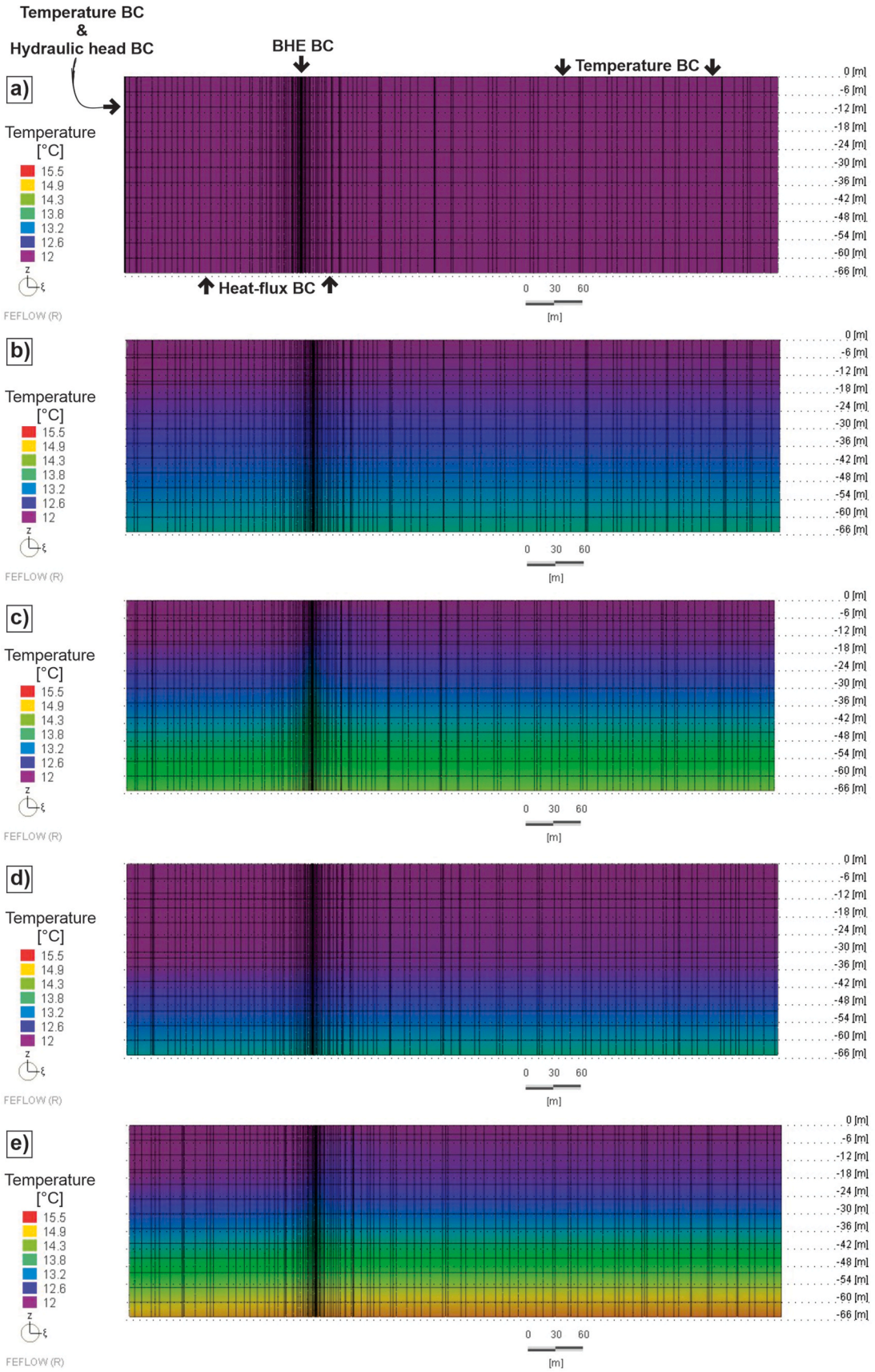

Fig. 4. Numerical model cross-sections with static temperature distribution before transient simulation for a) Sava Basin with BCs used, also for other basins, b) Savinja Basin, c) Krško Basin, d) Drava Basin, and e) Mura Basin.

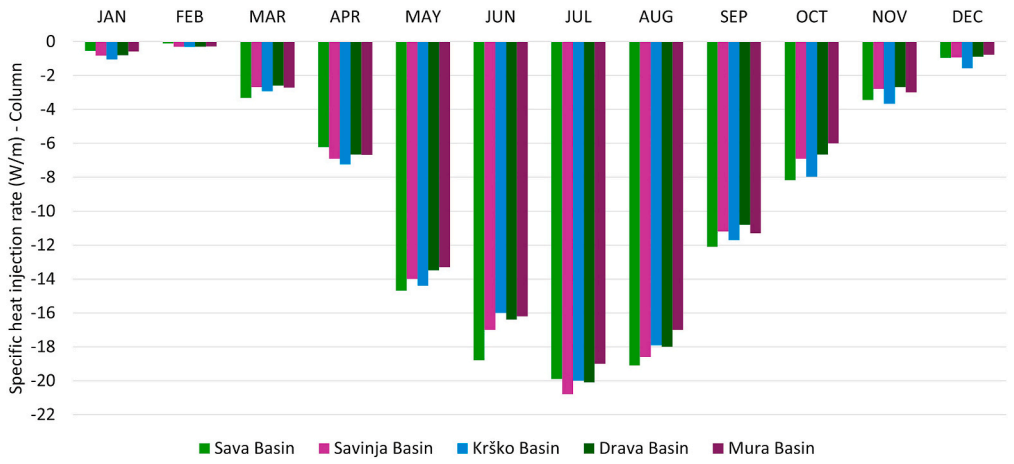

Fig. 5. Simulated specific heat injection rate of case study locations when considering maximum working fluid temperature of 24 °C (Scenario 8).

of heat that can be injected without exceeding the heat carrier temperature threshold 24 °C.

The simulations showed that the same amount of injected heat resulted in temperature fluctuations of ±2 °C in the maximum temperature of the heat carrier fluid in different case study locations after 30 years of BHE operation (Table 4). It is evident that the simultaneous injection of 33,455 kWh and attainment of the maximum temperature of 24 °C with the two 50 m deep borehole heat exchangers is not a viable option. If the condition of the maximum 24 °C of the heat carrier fluid is accounted for, the injection of between 6100 kWh and 5500 kWh (scenario 8) is the maximum possible heat input (Fig. 6).

The lowest maximum temperature for the heat carrier fluid was simulated in the Sava Basin (73 °C). To achieve a maximum heat carrier fluid temperature of 24 °C, it was necessary to reduce the annual cooling load by two-thirds, to 6100 kWh. Conversely, the highest maximum heat carrier fluid temperature was observed in the Mura Basin, with a value of 76 °C when 33,455 kWh was injected. To achieve a limit for heat carrier fluid temperature of 24 °C, the annual cooling load for the Mura Basin was reduced to 5500 kWh.

3.2. Numerical modeling

We ran three different simulations for the 5 case study sites, where SC1 represents the annual energy loads determined with scenario 8 in analytical modeling, SC2 represents the maximum heat carrier fluid temperature set to 24 °C, and SC3 represents the maximum annual energy load set to 33,455 kWh. It can be observed in the SC1 simulations that the inclusion of groundwater flow in calculations increases the possible amount of injected heat in comparison to the analytical simulations. The maximum temperatures of the heat carrier fluid after 30 years of simulation were observed to be between 13 and 16 °C (Fig. 7a). The lowest temperature of 13 °C was observed in the Sava Basin, despite

Table 4
Heat carrier fluid temperatures after 30 years for 7 scenarios with different amount of injected heat.

Nb. of simulation	Cooling (kWh)	Simulated temperatures (°C)				
		Sava Basin	Savinja Basin	Krško Basin	Drava Basin	Mura Basin
1	33,455	73	77	74	77	76
2	33,000	72	76	73	76	75
3	30,000	67	70	68	71	70
4	25,000	58	61	59	61	60
5	20,000	49	51	50	51	51
6	15,000	40	42	41	42	42
7	10,000	31	32	31	32	32

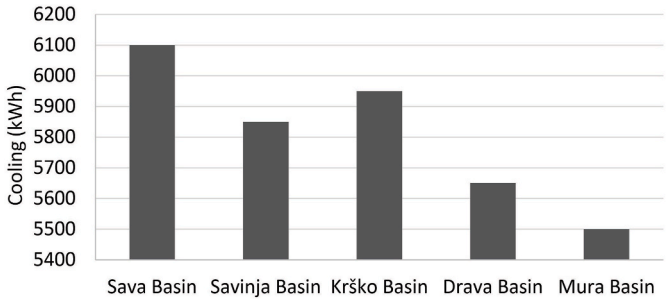

Fig. 6. The maximum possible injected amount of heat for 30 years considering the heat carrier fluid temperature limit of 24 °C.

the injection of the highest amount of heat obtained through analytical modeling (6100 kWh). This is related to the high groundwater flow velocity (7.2 m/day), which results in the flushing away some of the injected heat, as also observed in the study of Chiasson et al. [32]. In general, it can be observed that as the thickness of the aquifer increases and the groundwater velocity increases, the heat carrier fluid temperature decreases, thereby allowing for the injection of a greater quantity of heat. The groundwater flow transfers the thermal plume and restores temperature to the natural background of the aquifer.

In the SC2 simulations, the highest quantity of injected heat after 30 years of simulation is observed in the Sava basin, with a total of 57 MWh, resulting in a maximum heat carrier fluid temperature of 24 °C (Fig. 7b). The lowest quantity of injected heat is observed in the Savinja Basin, with a value of 17 MWh. This is despite the groundwater flow velocity and aquifer thickness being slightly higher than those observed in the Krško Basin (Fig. 7b). This difference is probably related to the variations in geology and, consequently, in thermal parameters, which are illustrated in Fig. 3. The Savinja Basin contains a greater proportion of marly rocks beneath the aquifer. In contrast, the Krško Basin comprises predominantly saturated sand and clay. Consequently, the latter can accumulate more heat (2.2 MWh more).

Our conservative temperature limit for the heat carrier fluid is 24 °C, as demonstrated in the SC2 simulations. The Savinja Basin example confirms this, with a maximum heat carrier fluid temperature of 24 °C (Fig. 8b – Savinja Basin PI), although the corresponding grout temperature is between 17.8 °C and 22.2 °C (Fig. 8b – Savinja Basin G). Also, from the 2D surface view, we can observe that 2 m away from the bottom of the BHE, the subsurface temperature is 15.2 °C. At a distance of 5 m, it drops slightly to 14.2 °C. These results indicate that the thermal impact on the surrounding soil is minimal. Therefore, future considerations should include the possibility of increasing the recommended

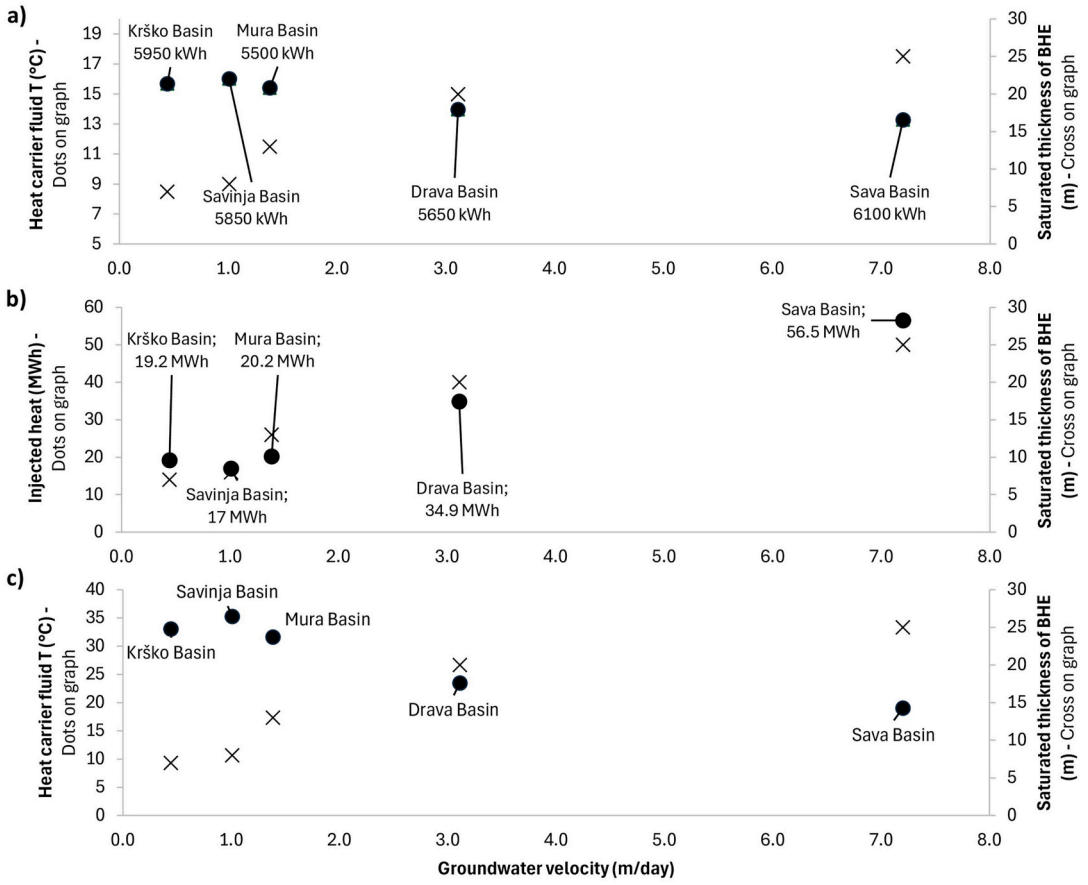

Fig. 7. Results of three scenarios after 30 years of simulation; **a)** Maximum heat carrier fluid temperatures obtained with the SC1 simulation; **b)** The maximum quantity of heat that can be injected without exceeding the temperature limit of the heat carrier fluid, which is 24 °C; **c)** Maximum heat carrier fluid temperatures obtained with the SC3 simulation. A maximum annual energy value was set at 33,455 MWh.

temperature of the heat carrier fluid.

The temperature trend of the heat carrier fluid in the SC3 simulations after 30 years of simulation is similar to that observed in the SC1 simulations. In general, the values are higher, ranging between 19 °C and 35 °C, in comparison to the SC1 simulations. The temperature of the heat carrier fluid was below 24 °C in only two locations, namely the Drava and Sava Basins. In the remaining three case study locations, the heat carrier temperature exceeded 30 °C after 30 years of operation (Fig. 7c). This is attributable to the thinner aquifer, in comparison to the Drava and Sava Basins, and the fact that the injected heat is not flushed away. Consequently, the heat carrier fluid temperature limit of 24 °C is reached and exceeded faster.

The influence of groundwater flow is evident when observing the temperature profiles of borehole heat exchangers across case studies at all three scenarios. In nearly all cases, a difference can be observed between the temperature of the pipe-in (PI) and pipe-out (PO) in comparison to the temperature of the grout (G) (Fig. 8). This indicates that the ground temperature (grout) is not identical to the heat carrier fluid temperature (pipe-in, pipe-out) and is, therefore, less affected by overheating. The difference between these two temperatures is higher in the aquifer zone and when a greater quantity of heat is injected underground, resulting in a faster rise in pipe temperature than in the surrounding environment. In general, the grout temperature profiles align with the layers delineated in conceptual models (Fig. 3), indicating only moderate temperature increases in aquifers. The aquifers reach their bottoms at 14 m in the Savinja and Krško Basins, 16 m in the Mura Basin, and 32 m in the Drava Basin. A sharp transition into less permeable layers is evident there.

The highest temperatures of the heat carrier fluid are observed in the case study location Savinja Basin, when the scenario SC3 is simulated (Fig. 8c), due to the predominant conduction over convection. The aquifer here is only 8 m thick, with 36 m of marly rocks without significant groundwater flow (Fig. 3). On the temperature profiles, we can also observe a slight temperature decrease at the end of the BHE (last node of BHE), which is related to the border effect at the bottom of BHE caused because of the pipe loop that enhances the heat transfer and decreases observed temperature.

The spatial distribution of the thermal plume varies depending on the depth at which it is observed, the case study location, and the scenario (Fig. 9). Therefore, Fig. 8 is supplemented with an example in Fig. 9. For the worst-case scenario (e. g. Savinja Basin, scenario SC3) in the bottom of the aquifer, the thermal plume extends in the groundwater flow direction with a maximum length of 55 m and a maximum width of 21 m (if observing the background temperature difference for more than 1 °C). The thermal plume dimensions at the bottom of the BHE are significantly larger, measuring 165 m in length and 112 m in width. The thermal plume is still oriented towards the groundwater flow direction due to the influence of the upper parts of the BHE. While the dimensions of a warm thermal plume in the worst-case scenario have a considerable spatial distribution, it is important to note that agricultural facilities, such as cold storage facilities, are typically large in size. Therefore, it is unlikely that thermal impacts will affect neighboring plots, provided that the BHE is situated at an appropriate distance from the plot border. The dimensions of the thermal plume in Fig. 9 can be related to the temperature profile of the Savinja basin (G) in Fig. 8c. The temperature profile in Fig. 8 shows temperature values in the grout that are only one point in the 2D surface view in Fig. 9. The latter complements Fig. 8 by also showing the temperature distribution in the vicinity of the BHE.

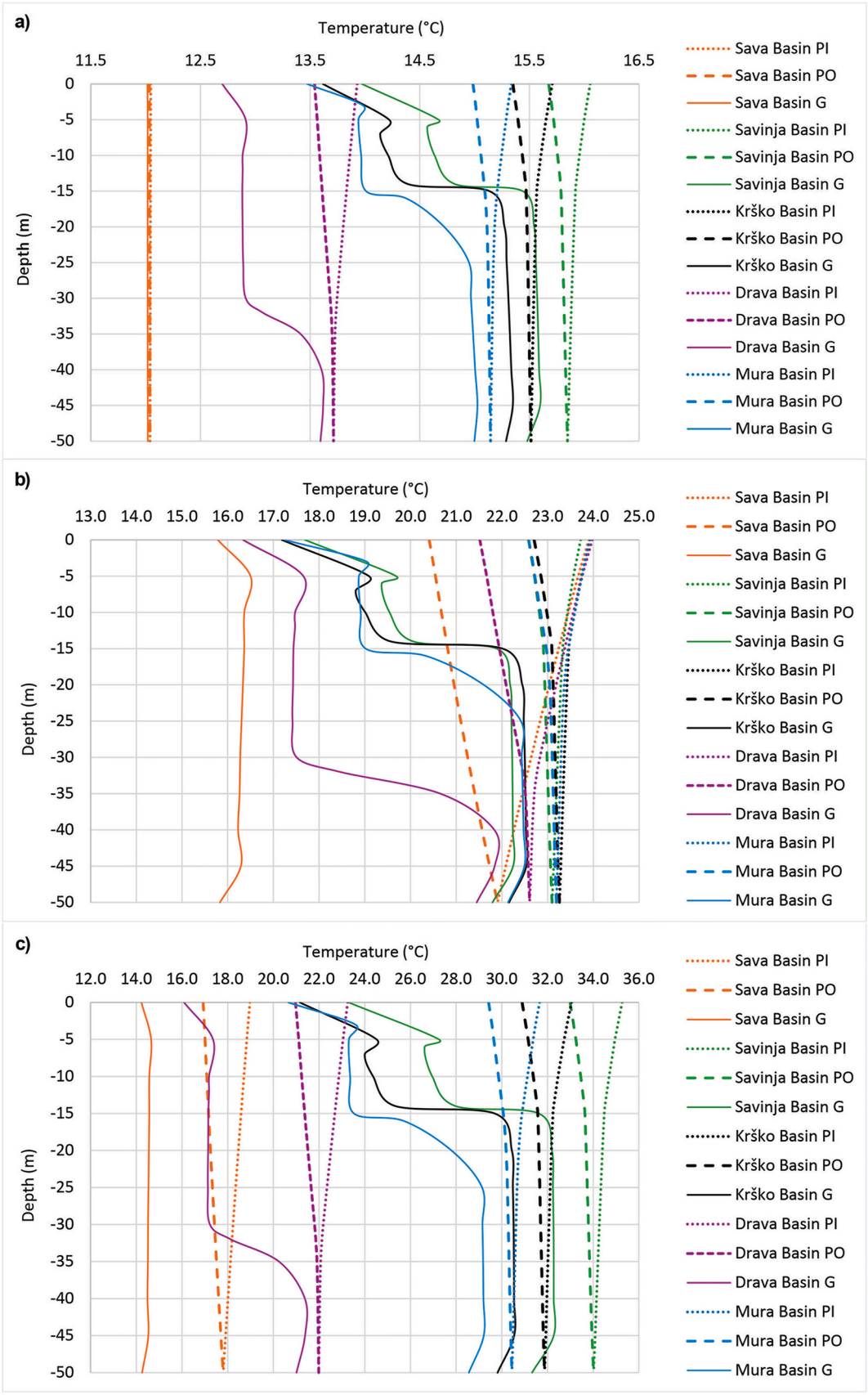

Fig. 8. The temperature profiles of Pipe-in flow (PI), Pipe-out flow (PO), and Grout (G) for the summer season, after 30 years of operation for scenarios a) SC1, b) SC2 and c) SC3.

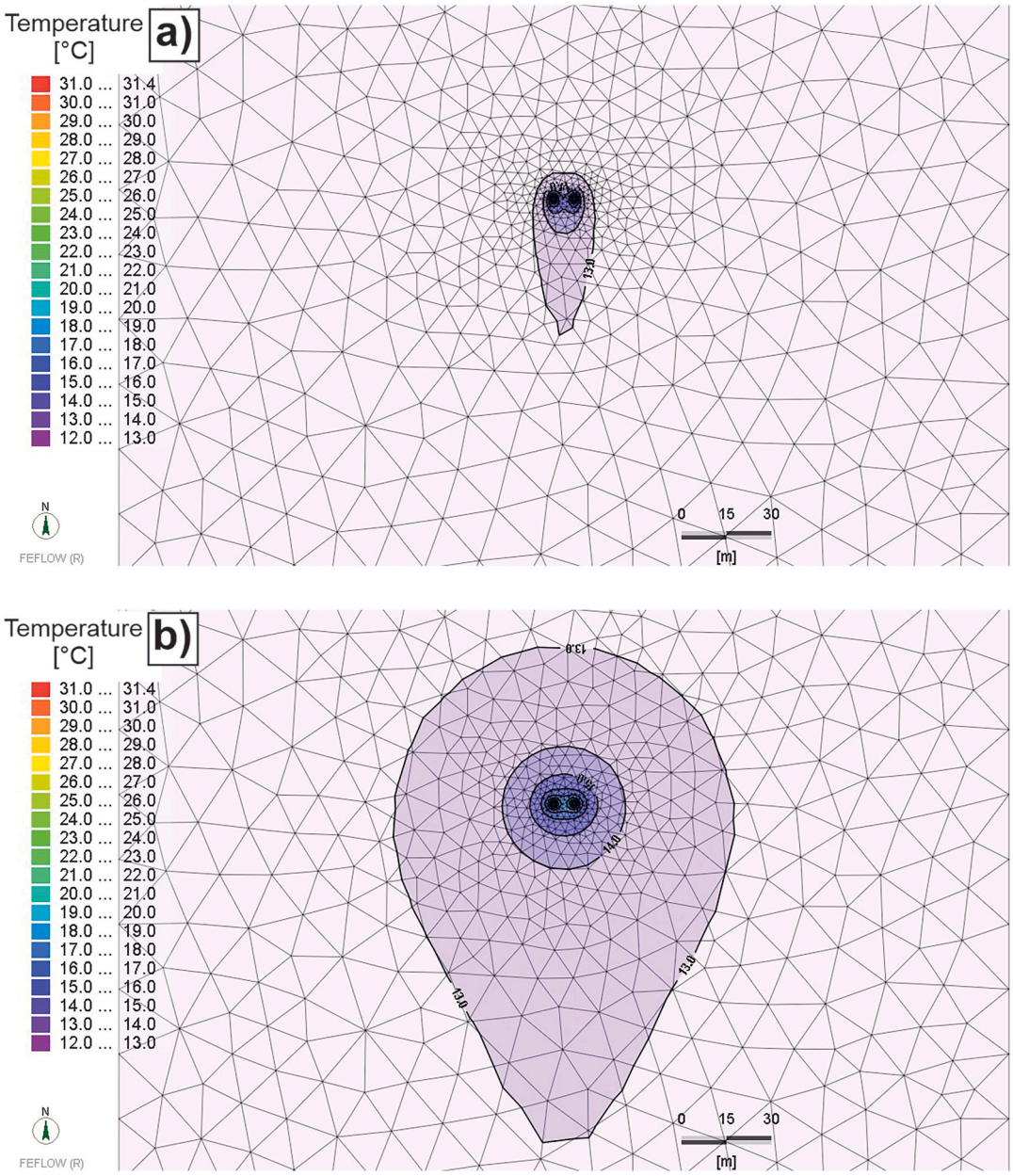

Fig. 9. Thermal plume in the Savinja Basin scenario SC3; a) at the bottom of the aquifer, b) at the bottom of the BHE.

3.3. Comparison

A comparison of the possible amount of injected heat with the analytical model EED and the numerical model FEFLOW confirmed that it is possible to inject more heat if the groundwater flow is present [32, 57,58]. The groundwater flow flushes the heat and restores the groundwater temperature to its natural background more quickly. However, it was necessary to ascertain the magnitude of this difference for the five case study locations. As can be seen from Table 5, groundwater flow contributes to a 926 % increase in the possible amount of injected heat (from 6100 kWh in conductive conditions to 56,500 kWh in convective conditions) in the Sava Basin, with the maximum heat carrier fluid temperature set at 24 °C. The potential increase in the quantity of heat that can be injected at the remaining four locations is significant, in comparison to the scenario involving conductive conditions. An increase of 291 % was observed in the Savinja Basin, while a maximum increase of 367 % was observed in the Mura Basin. In the SC3 scenario, a theoretical amount of heat (e.g., 33,455 kWh) was injected.

Table 5
Calculated maximum heat carrier fluid temperatures after 30 years by analytical (EED) and numerical (FEFLOW) methods for 3 scenarios of injected heat.

	EED	Scenario	FEFLOW
Sava Basin	6100 kWh = 24 °C	SC1	6100 kWh = 13 °C
	56,500 kWh = 114 °C	SC2	56,500 kWh = 24 °C
	33,455 kWh = 73 °C	SC3	33,455 kWh = 19 °C
Savinja Basin	5850 kWh = 24 °C	SC1	5850 kWh = 16 °C
	17,000 kWh = 45 °C	SC2	17,000 kWh = 24 °C
	33,455 kWh = 77 °C	SC3	33,455 kWh = 35 °C
Krško Basin	5950 kWh = 24 °C	SC1	5950 kWh = 16 °C
	19,200 kWh = 48 °C	SC2	19,200 kWh = 24 °C
	33,455 kWh = 74 °C	SC3	33,455 kWh = 33 °C
Drava Basin	5650 kWh = 24 °C	SC1	5650 kWh = 14 °C
	34,900 kWh = 80 °C	SC2	34,900 kWh = 24 °C
	33,455 kWh = 77 °C	SC3	33,455 kWh = 23.5 °C
Mura Basin	5500 kWh = 24 °C	SC1	5500 kWh = 15 °C
	20,200 kWh = 51.5 °C	SC2	20,200 kWh = 24 °C
	33,455 kWh = 76 °C	SC3	33,455 kWh = 32 °C

It is worth mentioning that groundwater flow is quite high at all sites in our case studies, ranging from 0.4 m/day to 7.2 m/day. This means that the outlet temperatures of the heat carrier fluid are influenced by it. Even at lower velocities than that, we can find examples, like from Guo et al. [59], that report a potential increase in average heat yield of 59.4 % from an increase in groundwater flow from 0.01 m/day to 0.59 m/day. Piipponnen et al. [31], for example, investigated the effects of groundwater flow in Estonia on different closed-loop configurations. They found that groundwater flow rates between 0.005 and 0.01 m/day have very little effect on energy yield. They therefore suggested that these velocities could be omitted from the modeling.

With the analytical modeling, we can conclude that the installation of two 50 m BHEs is insufficient, as the temperatures of the heat carrier fluid would reach between 73 °C and 77 °C, which exceeds the suggested thresholds. With the numerical modeling, even with the groundwater present, it is not possible to inject 33,455 kWh at Savinja, Krško, and Mura Basins (Table 5), which is related to their thicker aquifer (Fig. 3) and consequently predominant conduction over convection.

In the areas where groundwater flow-driven convection is not the dominant mechanism (such as in the Savinja, Krško and Mura Basins), we suggest that a combined cooling and heating approach is taken to enhance the thermal storage capacity on an annual basis. This means that the closed-loop system could be connected not only to the cold storage facility but also to nearby residential and commercial facilities that require heating during the winter season. With this combination, we could increase and make the most optimal use of shallow geothermal energy.

In the areas where groundwater flow and a deep aquifer are present (like in Sava Basin), combined heating and cooling will not result in an increase in the maximum amount of injected heat. The generated cold thermal plume in the winter time will be flushed away due to the groundwater flow, before the summer season. The temperature of the subsurface and groundwater will be balanced with the natural groundwater temperature.

Natural groundwater temperatures are increasing due to global warming of the surface [60]. The groundwater at the depth of the water table will warm up on average by 2.1 °C worldwide between 2000 and 2100 under a medium emissions pathway [60]. This will affect the shallow geothermal potential, reducing heating demands (also due to improved building insulation) and, on the other hand, making cooling less efficient, so recycling the subsurface heat will become more feasible.

It is essential that the authorities consider the establishment of a temperature limit for the heat injection process (e. g. in this paper, we set a temperature limit at of heat carrier fluid 24 °C). This is crucial to avoid any long-term negative impacts on microbial activity, groundwater chemistry and aquatic ecosystems. Only 18 of the 125 countries have temperature guidelines for drinking water [61], where the threshold is in the range of 15–34 °C, with a median of 25 °C. It is therefore crucial to make the most of the cooling potential of the shallow geothermal source by including combined heating and cooling where natural conditions allow. Different types of heat storage should not be a priori forbidden (e.g. high-temperature storage) but the allowed temperature limits should be individually based on the purpose of research and corresponding monitoring networks.

4. Conclusion

Our review of cold storage facilities in Slovenia showed a lack of recent research, with the majority of existing studies concentrating on the biological effects of the storage of fruits. Quite similar was noticed worldwide. Farm-hold cold storage facilities are predominantly situated in flatlands with alluvial intergranular aquifers with high groundwater flow. Denmark, Poland, and the Netherlands have similar hydrogeological conditions to Slovenia, but closed-loop systems prevail over open-loop systems in their case [4]. One of the benefits of applying closed-loop systems is that much less investigation of hydraulic, thermal, chemical and microbiological conditions of aquifers is needed, so planning phase is faster and cheaper, while installation phase costs depend on the number of needed boreholes. They also affect groundwater quality less as they are sealed off to prevent cross-contamination of water-bearing zones [1]. In Slovenia, proper construction of closed-loop systems is still an issue, however, we see them as the best alternative to use shallow geothermal energy in areas where open-loop systems are not possible due to low discharge or protection measures.

Consequently, the focus of this paper was only on vertical closed-loop systems.

The presented simulations of the analytically calculated maximum injected waste heat and the numerical simulations, including groundwater flow for the representative hydrogeological conditions of five Slovenian intergranular aquifers, revealed that the best natural conditions, if only cold production is planned, occur in the Sava Basin with significant groundwater flow and thick permeable layer. There, the possible injection of heat is greater than in areas without groundwater flow, yet after 30 years of operation, the heat carrier fluid still stays below 24 °C. The Savinja Basin has the lowest potential for heat injection due to thicker marly layer where heat is transferred predominately by conduction rather than convection. However, even there, the increase in possible heat injection is almost triple compared to what it would be without any presence of groundwater flow.

Our research yielded quantitative confirmation that the areas with groundwater flow are more favorable for restoring the underground temperature due to the injection of waste heat from cooling cold storages than the areas without groundwater. In the Sava Basin, the groundwater flow of 7.2 m/day contributed to an increase in potential heat injection of more than 900 %, if the maximum temperature of the heat carrier fluid is set at 24 °C. On the other hand, the groundwater flow of 1 m/day, which we observe in the Savinja Basin, contributed to a 170 % increase in the possible amount of injected heat. This means that groundwater flow significantly influences temperature distribution in the vicinity of boreholes, resulting in a shorter length of BHEs and the associated installation costs.

If only the cooling of cold storage facilities is planned, based on performed research, we suggest the use of closed-loop geothermal systems at:

- Areas with strong groundwater flow, to keep the capacity for heat injection.
- Boreholes, deeper than 50 m, to avoid effects of long-term subsurface temperature increase due to climate change, if this is possible.
- Implementing not just one borehole, but more (based on energy needs and local geological and hydrogeological conditions) will be needed to inject larger quantities of heat.

If cold storage is planned in agricultural facilities, we also advise searching for consumers of injected heat – i. e. heating demand in nearby buildings, as this dual approach significantly improves the capacity of the subsurface to cover the cooling and heating needs of the site.

CRediT authorship contribution statement

Simona Adrinek: Writing – original draft, Visualization, Validation, Software, Methodology, Investigation, Formal analysis, Conceptualization. **Joerg Prestor:** Writing – review & editing, Supervision, Methodology, Conceptualization. **Simona Pestotnik:** Writing – review & editing, Methodology, Investigation, Conceptualization. **Nina Rman:** Writing – review & editing, Supervision, Project administration, Methodology, Funding acquisition, Conceptualization.

Funding

The paper was prepared within the project V1-2213 GeoCOOL FOOD – Cold storage of food using shallow geothermal energy, funded as a

Targeted Research Program "Our Food, Rural Areas and Natural Resources" granted in 2022. Funds are granted by the Slovenian Research and Innovation Agency (ARIS) and the Ministry of Agriculture, Forestry and Food (MKGP). The authors acknowledge the financial support from the Slovenian Research and Innovation Agency (research core funding No. P1-0020 Groundwater and Geochemistry).

Declaration of competing interest

The authors declare that they have no known competing financial interests or personal relationships that could have appeared to influence the work reported in this paper.

References

[1] D. Banks, An Introduction to Thermogeology: Ground Source Heating and Cooling, second ed., Wiley-Blackwell, 2012 https://doi.org/10.1002/9781118447512.
[2] R. Al-Khoury, Computational Modeling of Shallow Geothermal Systems, CRC Press, 2012, https://doi.org/10.1201/b11462.
[3] K.P. Tsagarakis, Shallow geothermal energy under the microscope: social, economic, and institutional aspects, Renew. Energy 147 (2020) 2801–2808, https://doi.org/10.1016/j.renene.2019.01.004.
[4] S. Adrinek, M. Janža, R.M. Singh, Influence of geology, hydrogeology, and climate on ground source heat pump distribution in Slovenia and selected European countries, Resources 13 (3) (2024) 39, https://doi.org/10.3390/resources13030039.
[5] R. Valančius, J. Černeckienė, A. Jurelionis, L. Aresti, N. Rman, R.M. Singh, Analysis of the wider potential for heat pump and geothermal energy integration in traditional systems and grids, Energetika 69 (1) (2024) 16, https://doi.org/10.6001/energetika.2023.69.1.4.
[6] M. Kharseh, M. Al-Khawaja, M.T. Suleiman, Potential of ground source heat pump systems in cooling-dominated environments: residential buildings, Geothermics 57 (2015) 104–110, https://doi.org/10.1016/j.geothermics.2015.06.009.
[7] P. Christodoulides, A. Vieira, S. Lenart, J. Maranha, G. Vidmar, R. Popov, A. Georgiev, L. Aresti, G. Florides, Reviewing the modeling aspects and practices of shallow geothermal energy systems, Energies 13 (16) (2020) 4273, https://doi.org/10.3390/en13164273.
[8] A.A. Ahmed, M. Assadi, A. Kalantar, T. Sliwa, A. Sapińska-Śliwa, A critical review on the use of shallow geothermal energy systems for heating and cooling purposes, Energies 15 (12) (2022) 4281, https://doi.org/10.3390/en15124281.
[9] M.A.D. Larsen, S. Petrović, A.M. Radoszynski, R. McKenna, O. Balyk, Climate change impacts on trends and extremes in future heating and cooling demands over Europe, Energy Build. 226 (2020) 110397, https://doi.org/10.1016/j.enbuild.2020.110397.
[10] T. Abergel, C. Delmastro, Is Cooling the Future of Heating? International Energy Agency, Paris, 2020. Available on: https://www.iea.org/commentaries/is-cooling-the-future-of-heating.
[11] H. Boughanmi, M. Lazaar, S. Bouadila, A. Farhat, Thermal performance of a conic basket heat exchanger coupled to a geothermal heat pump for greenhouse cooling under Tunisian climate, Energy Build. 104 (2015) 87–96, https://doi.org/10.1016/j.enbuild.2015.07.004j.enbuild.2015.07.004.
[12] I. Al-Helal, A. Alsadon, S. Marey, A. Ibrahim, M. Shady, A. Abdel-Ghany, Geothermal energy potential for cooling/heating greenhouses in hot arid regions, Atmosphere 13 (1) (2022), https://doi.org/10.3390/atmos13010105.
[13] H. Pieskä, C. Wang, B. Nourozi, A. Ploskić, Q. Wang, Thermodynamic and thermal comfort performance evaluation of two geothermal high-temperature cooling systems in the mediterranean climate, J. Build. Eng. 56 (2022) 104738, https://doi.org/10.1016/j.jobe.2022.104738.
[14] P. Niemann, F. Richter, A. Speerforck, G. Schmitz, Desiccant-assisted air conditioning system relying on solar and geothermal energy during summer and winter, Energies 12 (16) (2019) 3175, https://doi.org/10.3390/en12163175.
[15] R. Singh, R. Thakur, N. Kalal, S. Parveen, D. Husain, R. Prakash, Energy efficient design of cold storage. International Conference on Sustainable Development, Online, United States, 2020. Available at: https://ic-sd.org/2020/11/21/proceedings-from-icsd-2020/.
[16] B. Pastakkaya, Performance analysis of a geothermal heat-powered resorption cooling system: a case study for cold storage of Apple fruit, Int. J. Low Carbon Technol. 18 (2023) 863–871, https://doi.org/10.1093/ijlct/ctad061.
[17] A. Galgaro, G. Dalla Santa, S. Cola, M. Cultrera, M. DeCarli, F. Conforti, P. Scotton, D. Viesi, M. Fauri, Underground warehouses for food storage in the dolomites (eastern alps – italy) and energy efficiency, Tunn. Undergr. Space Technol. 102 (2020) 103411, https://doi.org/10.1016/j.tust.2020.103411.
[18] D. Rajver, N. Rman, S. Pestotnik, A. Lapanje, M. Božič, S. Adrinek, J. Prestor, Pregled rabe geotermalne energije v sloveniji v letu 2023 - pomen plitve geotermalne energije se zvišuje (in Slovene), Mineralne surovine 20 (1) (2024) 156–174. Available on: https://www.geo-zs.si/index.php/za-javnost/publikacije2/periodi%C4%8Dne-publikacije/mineralne-surovine.
[19] Poslovna skupnost za sadje, krompir, vrtnine Slovenije. 1991. *Hladilnice v Sloveniji.* Poslovni odbor za hladilničarstvo (in Slovene, German and Italian), Ljubljana, p. 32.Slovenije, 1991.
[20] M. Kovačič, Izkoriščanje odpadne toplote hladilnice sadja: diplomsko delo (in Slovene), University of Maribor, Faculty of Mechanical Engineering, Maribor, 2001, p. 75.
[21] K. Cehte, Analiza delovanja hladilnice sadja in njena posodobitev: diplomsko delo (in Slovene), University of Ljubljana, Faculty of Mechanical Engineering, Ljubljana, 2016, p. 50.
[22] G. Dernovšek, Senzorji za analizo atmosfere v skladiščnih hladilnicah za sadje: diplomsko delo (in Slovene), University of Maribor, Faculty of Electrical Engineering and Computer Science, Maribor, (2008,) p.83. Available on: https://dk.um.si/Dokument.php?id=6623.
[23] A. Korošec, Ekonomska analiza investicije hladilnice za sadje: magistrsko delo (in Slovene), University of Maribor, Faculty of Agriculture and Life Sciences, Maribor, 2007, p. 101.
[24] M. Hadžić, Upravičenost vzpostavitve distribucijskega centra za sadje in zelenjavo na območju Ivančne Gorice: magistrsko delo (in Slovene), University of Maribor, Faculty of Logistic, Celje, 2019, p. 84. Available on: https://dk.um.si/Dokument.php?id=132671.
[25] H. Kaučič, Primerjava senzoričnih lastnosti jabolk, skladiščenih v naravni in kontrolirani atmosferi: diplomsko delo (in Slovene), Education Centre Piramida, Maribor, (2008, p.73.).
[26] S.E. Dehkordi, B. Olofsson, R.A. Schincariol, Effect of groundwater flow in vertical and horizontal fractures on borehole heat exchanger temperatures, Bull. Eng. Geol. Environ. 74 (2) (2015) 479–491, https://doi.org/10.1007/s10064-014-0626-4.
[27] M.H. Mueller, P. Huggenberger, J. Epting, Combining monitoring and modelling tools as a basis for city-scale concepts for a sustainable thermal management of urban groundwater resources, Sci. Total Environ. 627 (2018) 1121–1136, https://doi.org/10.1016/j.scitotenv.2018.01.250.
[28] G. Attard, P. Bayer, Y. Rossier, P. Blum, L. Eisenlohr, A novel concept for managing thermal interference between geothermal systems in cities, Renew. Energy 145 (2020) 914–924, https://doi.org/10.1016/j.renene.2019.06.095.
[29] R. Perego, G. Dalla Santa, A. Galgaro, S. Pera, Intensive thermal exploitation from closed and open shallow geothermal systems at urban scale: unmanaged conflicts and potential synergies, Geothermics 103 (2022) 102417, https://doi.org/10.1016/j.geothermics.2022.102417.
[30] A. Previati, J. Epting, G.B. Crosta, The subsurface urban heat island in milan (italy) - a modeling approach covering present and future thermal effects on groundwater regimes, Sci. Total Environ. 810 (2022) 152119, https://doi.org/10.1016/j.scitotenv.2021.152119.
[31] K. Piipponen, A. Soesoo, T. Arola, H. Bauert, S. Tarros, Impacts of groundwater flow on borehole heat exchangers: lessons learned from Estonia, Renew. Energy 237 (2024) 121448, https://doi.org/10.1016/j.renene.2024.121448.
[32] A.D. Chiasson, S.J. Rees, J.D. Spitler, Preliminary assessment of the effects of groundwater flow on closed-loop ground-source heat pump systems, ASHRAE Transactions 106 (2000).
[33] A. Angelotti, L. Alberti, I. La Licata, M. Antelmi, Energy performance and thermal impact of a borehole heat exchanger in a sandy aquifer: influence of the groundwater velocity, Energy Convers. Manag. 77 (2014) 700–708, https://doi.org/10.1016/j.enconman.2013.10.018.
[34] S.E. Dehkordi, R.A. Schincariol, Effect of thermal-hydrogeological and borehole heat exchanger properties on performance and impact of vertical closed-loop geothermal heat pump systems, Hydrogeol. J. 22 (1) (2014) 189–203, https://doi.org/10.1007/s10040-013-1060-6.
[35] F. Deng, W. Li, P. Pei, L. Wang, Y. Ren, Study on design and calculation method of borehole heat exchangers based on seasonal patterns of groundwater, Renew. Energy 220 (2024) 119711, https://doi.org/10.1016/j.renene.2023.119711.
[36] A. Previati, G. Crosta, On groundwater flow and shallow geothermal potential: a surrogate model for regional scale analyses, Sci. Total Environ. 912 (2024) 169046, https://doi.org/10.1016/j.scitotenv.2023.169046.
[37] M. Bonte, W.F.M. Röling, E. Zaura, P.W.J.J. van der Wielen, P.J. Stuyfzand, B. M. van Breukelen, Impacts of shallow geothermal energy production on redox processes and microbial communities, Environ. Sci. Technol. 47 (24) (2013), https://doi.org/10.1021/es4030244.
[38] C. Griebler, H. Brielmann, C.M. Haberer, S. Kaschuba, C. Kellermann, C. Stumpp, F. Hegler, D. Kuntz, S. Walker-Hertkorn, T. Lueders, Potential impacts of geothermal energy use and storage of heat on groundwater quality, biodiversity, and ecosystem processes, Environ. Earth Sci. 75 (20) (2016) 1391, https://doi.org/10.1007/s12665-016-6207-z.
[39] S. Haehnlein, P. Bayer, P. Blum, International legal status of the use of shallow geothermal energy, Renew. Sustain. Energy Rev. 14 (9) (2010) 2611–2625, https://doi.org/10.1016/j.rser.2010.07.069.
[40] V. Somogyi, V. Sebestyén, G. Nagy, Scientific achievements and regulation of shallow geothermal systems in six European countries – a review, Renew. Sustain. Energy Rev. 68 (2017) 934–952, https://doi.org/10.1016/j.rser.2016.02.014.
[41] GeoZS, Geološki atlas Slovenije = Geological Atlas of Slovenia, in: M. Novak, N. Rman (Eds.), Geological Survey of Slovenia, Ljubljana, 2016.
[42] D. Rajver, Surface Heat Flux Density Map, 1: 100,000, Geological Survey of Slovenia, Ljubljana, 2015. Available on: https://egeologija.si/.
[43] J. Prestor, S. Pestotnik, D. Rajver, J. Jež, D. Gerčar, K. Klančič, J. Svetina, Map of Temperature Distribution on the Surface of Solid Ground 1: 100,000, Geological Survey of Slovenia, , Ljubljana, 2018. Available on: https://egeologija.si/.
[44] D. Rajver, Geothermal Map – Expected Temperatures at a Depth of 100 m, 1: 100,000, Geological Survey of Slovenia,, Ljubljana, 2019. Available on: https://egeologija.si/.
[45] D. Rajver, S. Adrinek, Overview of the thermal properties of rocks and sediments in Slovenia, Geologija 66 (1) (2023) 125–150, https://doi.org/10.5474/geologija.2023.005.

[46] D. Rajver, S. Pestotnik, J. Prestor, Examples of the assessment of temperatures on the surface of solid ground in the design of the shallow geothermal energy extractions, Geologija 62 (1) (2019) 103–122, https://doi.org/10.5474/geologija.2019.005.
[47] N. Molina-Giraldo, P. Bayer, P. Blum, Evaluating the influence of thermal dispersion on temperature plumes from geothermal systems using analytical solutions, Int. J. Therm. Sci. 50 (7) (2011) 1223–1231, https://doi.org/10.1016/j.ijthermalsci.2011.02.004.
[48] B. Piga, A. Casasso, F. Pace, A. Godio, R. Sethi, Thermal impact assessment of groundwater heat pumps (GWHPs): rigorous vs. simplified models, Energies 10 (9) (2017), https://doi.org/10.3390/en10091385.
[49] Blocon, EED manual - Version 4. https://buildingphysics.com/, 2016.
[50] P. Eskilson, Thermal analysis of heat extraction boreholes, Ph.D. Thesis, University of Lund, Department of Mathematical Physics Sweden (1987) p. 81.
[51] G.A.J. Hellstrom, Ground Heat Storage, Thermal Analyses of Duct Storage Systems, Ph.D. Thesis,University of Lund, Department of Mathematical Physics (1991) 262.
[52] GeoCOOL-FOOD, Analiza naravnih danosti za karakterizacijo izbranega pilotnega območja (DP3). Project V1-2213 »GeoCOOL FOOD - Hladno skladiščenje hrane z rabo plitve geotermalne energije«. GeoZS, Ljubljana, 2025 [in preparation].
[53] ARSO, Značilno Meteorološko Leto, Slovenian Environment Agency, Ljubljana, 2024 Available at: https://meteo.arso.gov.si/met/sl/climate/tables/test_ref_year/.
[54] H.J.G. Diersch, FEFLOW: Finite Element Modeling of Flow, Mass and Heat Transport in Porous and Fractured Media, Springer, Berlin, Heidelberg, 2014, p. 996.
[55] H.J.G. Diersch, D. Bauer, W. Heidemann, W. Rühaak, P. Schätzl, Finite element modeling of borehole heat exchanger systems, Comput. Geosci. 37 (8) (2011) 1122–1135, https://doi.org/10.1016/j.cageo.2010.08.003.
[56] P. Eskilson, J. Claesson, Simulation model for thermally interacting heat extraction boreholes, Numer. Heat Tran. 13 (2) (1988) 149–165.
[57] N. Molina-Giraldo, P. Blum, K. Zhu, P. Bayer, Z. Fang, A moving finite line source model to simulate borehole heat exchangers with groundwater advection, Int. J. Therm. Sci. 50 (12) (2011) 2506–2513, https://doi.org/10.1016/j.ijthermalsci.2011.06.012.
[58] M. Samson, J. Dallaire, L. Gosselin, Influence of groundwater flow on cost minimization of ground coupled heat pump systems, Geothermics 73 (2018) 100–110, https://doi.org/10.1016/j.geothermics.2018.01.003.
[59] L. Guo, J. Zhang, Y. Li, J. McLennan, Y. Zhang, H. Jiang, Experimental and numerical investigation of the influence of groundwater flow on the borehole heat exchanger performance: a case study from tangshan, China, Energy Build. 248 (2021) 111199, https://doi.org/10.1016/j.renene.2025.122539.
[60] S.A. Benz, K. Menberg, P. Bayer, B.L. Kurylyk, Shallow subsurface heat recycling is a sustainable global space heating alternative, Nat. Commun. 13 (1) (2022) 3962, https://doi.org/10.1038/s41467-022-31624-6.
[61] World Health Organization, A Global Overview of National Regulations and Standards for drinking-water Quality, World Health Organization, Geneva, 2021. Available on: https://iris.who.int/handle/10665/350981.